Prospects of the Variational Approach

Hans Hersbach

European Centre for Medium-Range Weather Forecasts
Shinfield Park, Reading, RG2 9AX, UK

Abstract

At ECMWF, the assimilation of altimeter data into the ocean wave model (WAM cycle 4) is based on a sequential method. If a promotion to a variational method, such as the ECMWF 4D-Var system used for the atmosphere, is to be explored, the adjoint of the full WAM cycle 4 model is required. It was derived some years ago at KNMI. Its performance and capabilities for an inverse modelling application were reported to the literature. In that work it was found that both the wind input and the white-capping source term should be reduced with respect to the best estimater. In this best estimate, the white capping dissipation is proportional to the square of the wave steepness. Furthermore, it was suggested that this dependency should be increased to a cubic one. A concise description of those results will is presented.

1. Introduction

Since 29 June 1998, the ECMWF atmospheric model and the ocean-wave model (WAM cycle 4, see Komen et al. 1994) have been two-way coupled. Besides the generation of ocean waves by the forcing atmospheric 10m winds, the roughness length of the sea surface depends on its sea state, which in turn influences the flow in the atmospheric boundary layer (Janssen 1989, 1991). For the data assimilation part of the ECMWF forecast system, however, this two-way coupling is not completely consistent. Firstly, observations are assimilated into the atmospheric component using the 4D-Var variational approach (Rabier et al., 2000), retaining the two-way coupling only in the trajectory calculations. Then for the final trajectory, altimeter data are assimilated into the ocean-wave component using the sequential method of optimum interpolation (see Bidlot in this volume). In this way wind information obtained from observations assimilated in the atmospheric component are passed on to the wave model. On the other hand, in the final trajectory, wave information obtained from altimeter data are partially fed back to the atmosphere through the wave-induced stress. However, altimeter wave information can also flow in the opposite direction: wave height observations provide some information on the (local) winds that have generated these waves (which applies for a one-way coupled system as well). Such information flow is neglected in the present assimilation system. This may introduce inconsistencies between the forcing wind fields provided by the atmospheric analysis, and the wave observations. In this case, the resulting wave increments could subsequently be overruled by inconsistent forcing wind fields.

One possible way this information flow could be taken into account is to first generate some pseudo surface wind observations from the wave observations. These could then be added to the 4D-Var cost function. The resulting analysis winds are then expected to be more consistent with the wave observations. The most suitable tools to determine such information require the adjoint to the part of the model that translates winds into waves, i.e., the adjoint of the WAM cycle 4 model.

Alternatively, one could regard the atmosphere and ocean waves as one complete system, without making an 'artificial' separation between the two sub-systems. In addition to the sensitivity from the winds to the waves, a 4D-Var assimilation of such a system will also account for the sensitivity from the waves to the winds via the wave-induced stress. This requires the adjoint of the wave model aswell. In theory, such a method would be the most consistent one. However, it might be difficult to implement and its additional value compared to a simpler scheme such as the presently used sequential set-up (optimum interpolation or possibly the introduction of an ensemble Kalman filter, see Evensen, 1997; Burgers et al., 1998) or the set-up including pseudo wind observations, might not be large.

If one of the above mentioned extensions to the present analysis system is to be explored, the adjoint of the WAM cycle 4 model is required. It was derived some time ago (Hersbach 1997) and as a first test, was used for an inverse modelling application (Hersbach 1998). The remainder of this presentation will give a concise description of that work.

2. The adjoint of WAM cycle 4

A technical complication of the adjoint method is that one has to derive the adjoint model first from the forward model equations. This can be quite a tedious operation. In the case of the WAM cycle 4 model, for instance, the derivation of the adjoint to the nonlinear interactions is very complex (performed by the las Heras, 1994).

Alternatively, one can derive an adjoint on computer code level. In this case one regards the computer source code that represents the numerical implementation of the model as the forward model. The adjoining of this can be performed line by line, and tools have been developed that automatize this procedure. Using such a tool, the adjoint model compiler (AMC, see Giering et. al. 1997), the adjoint of the full-dimensional WAM cycle 4 model (i.e. 2d in physical space, 2d in spectral space, plus time) was derived (Hersbach 1997). The resulting adjoint code, ADWAM, is only 70% slower than WAM cycle 4, and is efficient in the storage of the nonlinear trajectory. It can be used in realistic situations for the assimilation of wind fields, initial fields and model parameters. No restrictions in the dimensionality or complexity of the wave model had to be made. This is in contrast to previous work (De Valk and Calkoen 1989: second generation wave model; De las Heras 1992, 1994: one-grid point version; Barzel 1994: one-dimensional stationary wave model).

3. Application to inverse modelling

As a first application, ADWAM was used for inverse modelling, with the objective to gain more insight into the numerical values of several model parameters in the WAM cycle 4 source terms. The adjoint method is a very powerful tool to obtain this information, because it can trace back the sensitivities of the model results with respect to the model parameters.

Two adjoint runs were performed. For the first, both deep water fetch data, which were compiled by Kahma and Calkoen, and shallow water fetch data, which were obtained from Lake George (Australia) by Young and Verhagen, were considered simultaneously. The second adjoint run was performed for a storm which occurred in the North Sea in February 1993.

3.1 Fetch-limited growth

In order to study the case of shallow-water fetch-limited growth, Young and Verhagen (1996) performed an extensive experiment in Lake George (35.2S,149E), near Canberra, Australia. Lake George is approximately 20 km long and 10 km wide and has a flat bottom of about 2 m depth (see figure 1). A detailed description of the experiment can be found in Young and Verhagen (1996). The WAM

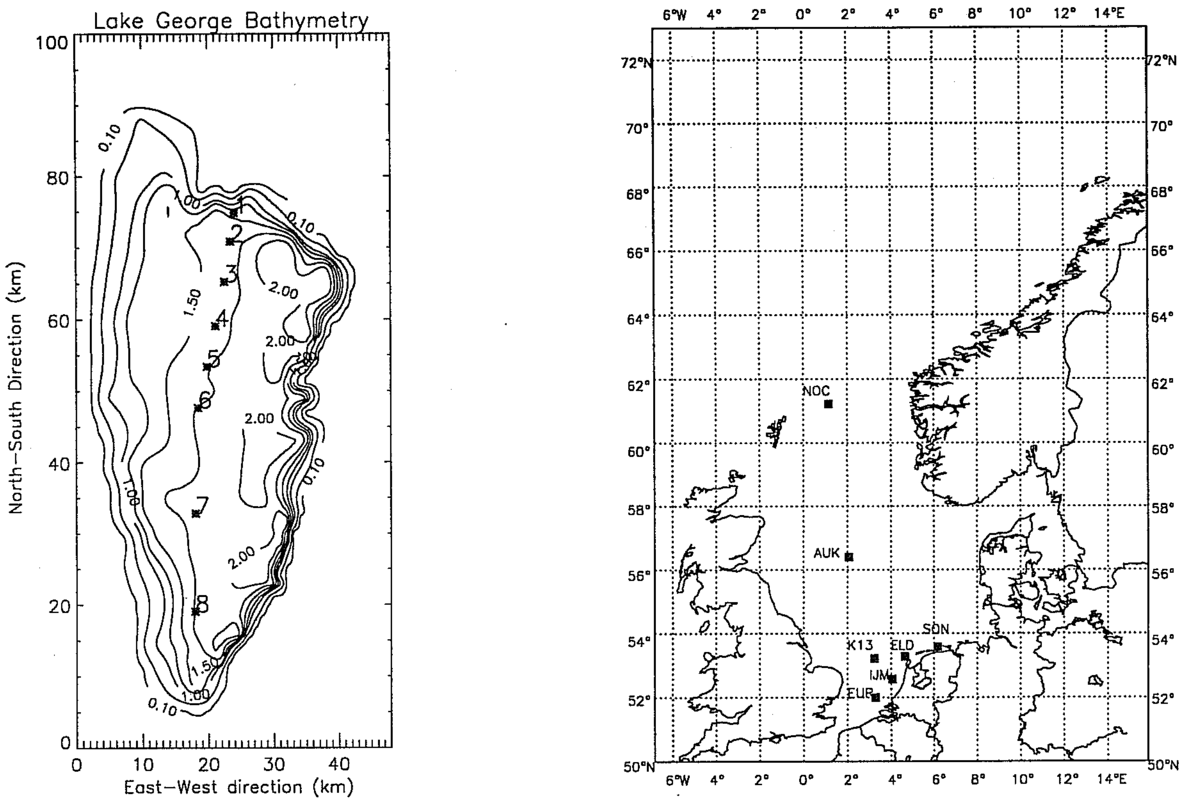

Figure 1: Left panel: Lake George bathymetry (meters) and station locations. Right panel: Wavec buoy locations in the North Sea. Only data from AUK, K13 and EUR were assimilated.

cycle 4 model was implemented on grid with a 1/80 degree = 1.39 km resolution, a time step of 180 s and a frequency range from 0.2 Hz - 2.0 Hz. To allow for this 'down scaling' an inconsistency in the u_*-scaling behaviour of WAM cycle 4 was restored first (Hersbach and Janssen 1999). At the east end of the Lake George grid one extra north-south line of 15 'sea' points with infinite depth was added. Each point of this line was chosen to be its own east-west neighbour. Therefore, in combination with a southern constant wind, this exactly mimics the situation of an infinite coast line.

The overall strengths of the wind input (β_m), white-cap dissipation (C_{dis}) and bottom dissipation (C_{bot}) were optimized (see appendix for definitions). In addition, the power dependency of the average wave steepness (D_s, see Eq.(9)) on S_{dis} was allowed to vary, because it was argued in Hersbach 1998 that this parameter could correct for a possible misfit in the dimensionless quantity $Y_p = H_s f_p^2/g$ It was shown to be rather insensitive to errors in the forcing wind field, and therefore a good indicator for possible model errors. In addition, the Lake George bathymetry was adapted. However, it was found not to lead to any significant changes and, therefore, will be disregarded in the following discussion. WAM cycle 4 model results for the 4 control variables: $\beta_m \to C_1\beta_m$, $C_{\text{dis}} \to C_2 C_{\text{dis}}$, $D_s \to C_3 D_s$ and $C_{\text{bot}} \to C_4 C_{\text{bot}}$ were compared to the available observations by means of the following cost function:

$$J(\vec{C}) = J_{\text{LG}}(\vec{C}) + J_{\text{KC}}(\vec{C}) + J_{\text{FG}}(\vec{C}), \tag{1}$$

The first part, relevant for Lake George, contains observed wave heights H^{LG}, their confidence levels

Quantity	Cvar	Default WAM	iteration # 4	Final fit
Strength S_{in}	C_1	1.0	0.78	0.79
Strength S_{dis}	C_2	1.0	1.03	0.63
Steepness S_{dis}	C_3	1.0	1.04	1.20
Strength S_{bot}	C_4	1.0	1.02	2.43
Cost function				
First-Guess	J_{FG}	0	6	21
Kahma-Calkoen	J_{KC}	1140	90	87
Lake George	J_{LG}	624	396	316
Total cost	J	1764	492	424

Table 1: Numerical values of the control variables, before and after optimization for the fetch-limited growth case.

$H^{\text{LG}}_{\text{max}}$, $H^{\text{LG}}_{\text{min}}$, and observed peak frequencies f^{LG}_p at the 8 stations (see figure 1):

$$J_{\text{LG}} = \sum_{i=\text{time, stations}} \sum \left(\frac{H^{\text{LG}}_i}{(H^{\text{LG}}_{\text{max}})_i - (H^{\text{LG}}_{\text{min}})_i} \right)^2 \left[\left(\frac{H^{\text{WAM}}_i - H^{\text{LG}}_i}{H^{\text{LG}}_i} \right)^2 + \left(\frac{f^{\text{WAM}}_{p,i} - f^{\text{LG}}_{p,i}}{f^{\text{LG}}_{p,i}} \right)^2 \right] \quad (2)$$

The second term in Eq.(1) accounts for deep-water fetch:

$$J_{\text{KC}} = 200 \sum_{i=\text{fetchline}} \left\{ 2 \left(\frac{E^{\text{WAM}}_i - E^{\text{KC}}_i}{E^{\text{KC}}_i} \right)^2 + \left(\frac{f^{\text{WAM}}_{p,i} - f^{\text{KC}}_{p,i}}{f^{\text{KC}}_{p,i}} \right)^2 \right\}, \quad (3)$$

where (see Hersbach 1998) E^{KC} and f^{KC} are a combination of fetch limited growth curves determined by Kahma and Calkoen (1992) and Pierson-Moskowitz (1964). Finally, the confidence in the current estimate of the model parameters is expressed by $J_{\text{FG}} = 400(D_s - 2)^2$. No penalty on β_m and C_{dis} was imposed; it should be implicitly taken care of by the deep-water fetch constraint.

A 12-hourly period (June 9, 1993, 0000-1200 UT) with a northerly wind ($U_{10} \sim 5 - 8$m/s) and, therefore, 'long' fetch, was chosen for the optimization. Cost function (1) was minimized using ADWAM in combination with the package MUDOLOPT (Gilbert and Lemaréchal, 1989). The result after 25 iterations is displayed in Table 1.

There was a fast drop (from 1764 to 492) of the cost within a few iterations. It was mainly induced by an improved fit to the deep-water fetch relations. From then, effectively J_{LG} was minimized, with J_{KC} acting as a strong constraint forcing the relative strengths between wind-input and white-cap dissipation to proper deep-water fetch-limited growth curves. Similar values of the total cost were found for a range of combinations between S_{in} and S_{dis} (see figure 2). Fetch-limited growth alone is not able to determine their exact values. However, it seems likely that their strengths should be smaller than their default values. This is also true for the final fit: the wind-input is reduced by 21%, the white-cap dissipation by 37%. In this final fit, the bottom dissipation was increased considerably, suggesting that the Lake George bed material is more dissipative than the material near Silt, Germany, where the JONSWAP experiment was performed (Hasselmann et al, 1973). In addition, the values of the steepness parameter D_s was increased with 20%. The optimized set of parameters was tested for an independent period with westerly winds ($U_{10} \sim 5 - 15$m/s). Good results for the final fit were obtained. However, the parameter set at iteration # 4 gave rise to too

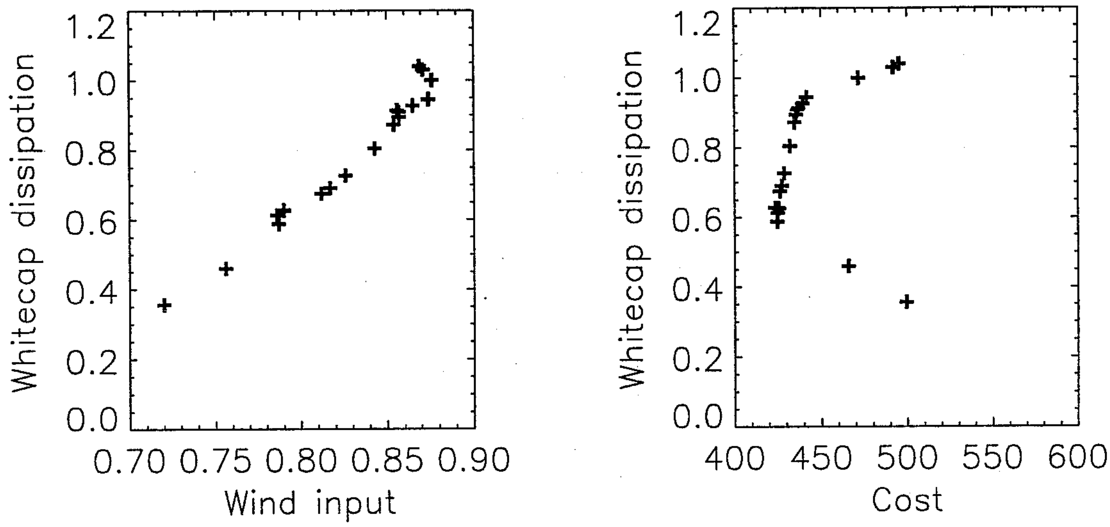

Figure 2: Scatter plot of the strength of the white capping versus the strength of the wind input (left panel), respectively the cost (right panel). Only points explored by the adjoint optimization that gave rise to a cost lower than 500 are displayed.

high waves, suggesting that only a strong dissipative force, like $S_{\rm bot}$ is capable of restricting the waves in a proper way.

3.2 The Wadden storm

The North Sea (see figure 1) constitutes a suitable environment in which the combination of deep and shallow water, and wind sea and swell can be studied simultaniously. It, therefore, provides a more demanding constraint on the strength of the individual sources. Especially it is expected that the absolute strengths of the wind input and white-cap dissipation can be better determined. This information is hidden in swell components, in which the wind input source term is not effective.

The Wadden storm (February 14-28 1993) was selected as the test period. It contained a situation with extreme wave conditions (up to 10m in the southern part of the North Sea). WAM cycle 4 was implemented on a grid running from 50.66^o N - 66.00^o N and from 7.00^o W - 8.00^o E, with a spatial resolution of 2/3 degree in the latitudinal direction and 1 degree in the longitudinal direction and a time step of 1800s. Deviations from model runs on larger and finer grids were found $\sim$ 10 cm in wave height only. In addition to the control variables β_m, $C_{\rm dis}$, D_s and $C_{\rm bot}$, the strength of the nonlinear interactions $C_{\rm nl}$, the parameters δ in $S_{\rm dis}$ and z_α in $S_{\rm in}$ (accounts for gustiness), were allowed to vary. The WAM cycle 4 model was forced with LAM winds (Kållberg, 1990) and the results were compared to Wavec buoys (provide directional information, see Kuik et al., 1988) by means of the cost function:

$$J(\vec{C}) = \sum_i 2N_i \left\{ \left(\frac{E_i - E_i^d}{E_i^d}\right)^2 + \left(\frac{f_{{\rm mean},i} - f^d_{{\rm mean},i}}{f_{{\rm mean},i}}\right)^2 + \left(\frac{\theta_{{\rm mean},i} - \theta^d_{{\rm mean},i}}{\pi}\right)^2 \right\}. \qquad (4)$$

Here E^d, $f^d_{\rm mean}$ and $\theta^d_{\rm mean}$ are the observed wave energy, mean frequency and mean direction of the Wavec buoys AUK, K13 and EUR (see figure 1). N is the number of degrees of freedom to convert the time series to energy spectra.

This cost function was optimized for the 2-day period February 19-21 1993, which was just before the maximum of the storm. A rather gradual convergence from $J = 128$ to a single minimum ($J = 66$, see

Quantity	Cvar	Default	Fit	Final value
β_{m}	C_1	1.0	1.07	$\beta_m = 1.28$
z_α	C_2	1.0	0.24	$z_\alpha = 0.0026$
Strength S_{nl}	C_3	1.0	0.73	$C_{\mathrm{nl}} = 0.73$
Strength S_{dis}	C_4	1.0	0.50	$C_{\mathrm{dis}} = 4.7\times10^{-5}$
δ in S_{dis}	C_5	1.0	0.61	$\delta = 0.31$
D_{s} in S_{dis}	C_6	1.0	1.51	$D_{\mathrm{s}} = 3.0$
Strength S_{bot}	C_7	1.0	1.20	$C_{\mathrm{bot}} = 0.0456$
Cost function	J	128	66	

Table 2: Numerical values of the control variables before and after optimization for the Wadden storm.

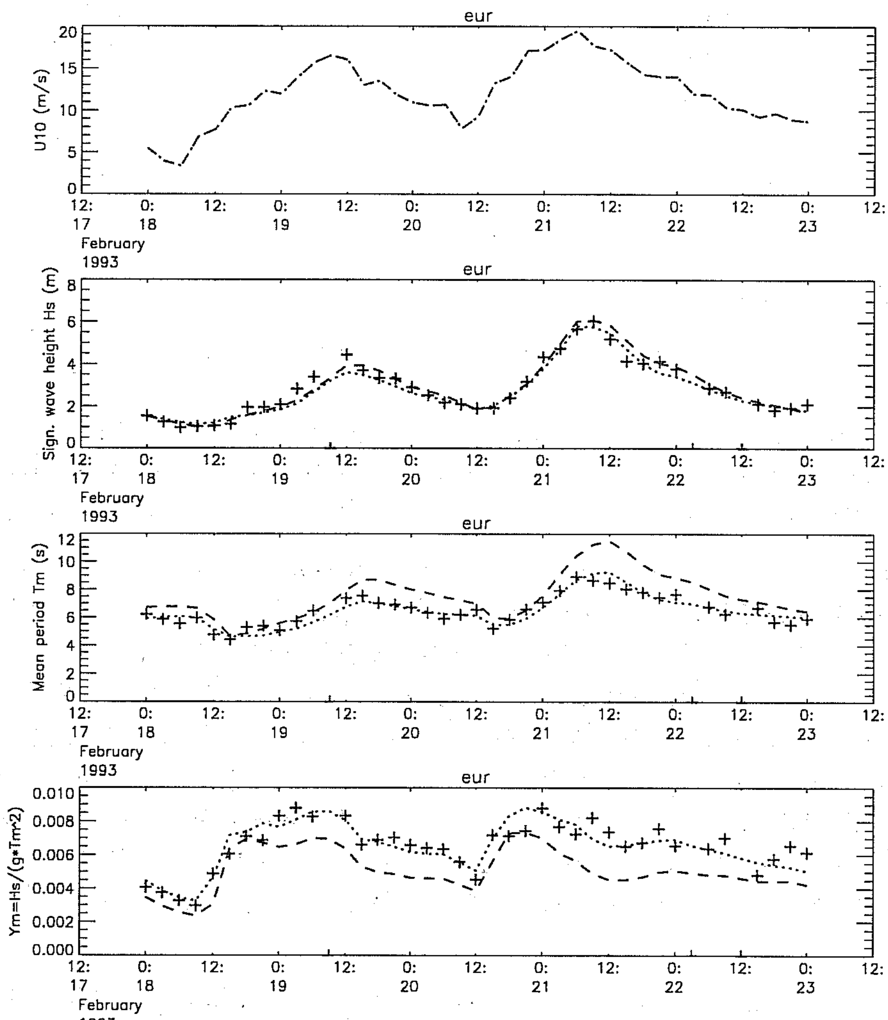

Figure 3: Validation of the optimized setting of the WAM model parameters for the EUR buoy. The wavec data are indicated by the pluses. The model results obtained from the default setting of WAM are represented by the dashed lines, while the results obtained from the optimal setting are given by the dotted lines. Only the period February 19-21 was used for the optimization.

Table 2) was observed. At the minimum, again white-cap dissipation was decreased (50%), but the integral strength β_m of the wind input was slightly increased (7%). However, the gustiness parameter was decreased significantly, and it was argued in Hersbach 1998 that this effectively reduce the wind input. The range of combinations of β_m and C_{dis} for which a comparable cost (below 70) was found, was much smaller than for the fetch-limited growth case. Indeed, the combination of wind-sea and swell for this more complex situation, seems to be more able to separate the several source terms. For EUR, the most southerly buoy used in the optimization, time series are given in figure 3 (for AUK and K13 similar results apply). From this it is seen that for the default setting of the WAM cycle 4 model (dashed), wave heights were quite well predicted. However, mean period (T_m) were overestimated. The dimensionless quantity $Y_m = H_s/(gT_m^2)$ can be shown to be rather insensitive to errors in the forcing wind fields. It was consistently underestimated for all three buoys (for EUR, see figure 3). This misfit is likely to originate from model errors. It is sensitive to the value of the steepness parameter D_s. Indeed, after optimization, the dependency of S_{dis} on average wave steepness is increased from a quadratic to a cubic one. The resulting fit for Y_m is excellent. This is also true for periods outside the optimization window. The bottom dissipation was increased by 20%. Finally, the strength of the nonlinear interaction was reduced by 27%. Its dependency on the cost was found to be small compared to the other source terms. The presence of its mechanism (redistribution of wave energy) might be more important than it precise strength.

4. Concluding remarks

The fetch-limited case was rerun for the fit obtained from (see Table 2) the Wadden storm, with the exception of C_{bot}. The deep-water growth curve for energy appeared to be 10% higher (which is probably well within the known accuracy), but the peak frequencies were basically the same. Almost identical results (both for f_p and H_s) were obtained for Lake George. Because of the more complex situation, the set of retuned parameters given by Table 2 is to be preferred. It leads to improved performance for both considered cases. However, such improvements were not reproduced for experiments for other periods and/or areas performed at KNMI and ECMWF.

Finally, it should be noted that the WAM cycle 4 contains many small discontinuities induced by the discretization. ADWAM is the exact gradient to the WAM cycle 4 source code. Therefore, it can happen (which was indeed observed) that the local correct gradient obtained by ADWAM does not represent the desired more global behaviour of the cost function. Research to resolve such discrepancies is required before the implementation of ADWAM in a assimilation scheme could be considered.

A. WAM cycle 4 source terms

In this appendix the WAM cycle 4 source terms are given. A comprehensive description may be found in Komen et al. (1994).

A.1 The wind input

$$S_{\text{in}} = \omega \frac{\rho_{\text{air}}}{\rho_{\text{water}}} \beta(x, z_0) x^2 F, \tag{5}$$

z_0 is the roughness length,

$$x = \left(\frac{u_*}{c_p} + z_\alpha \right) \cos(\theta - \phi), \quad z_\alpha = 0.011 \tag{6}$$

c_p is the phase speed, ω angular velocity and $\theta - \phi$ is the angle between wave propagation and wind direction. The function $\beta(x, z_0)$ is given by

$$\beta = \frac{\beta_m}{\kappa^2} \mu \ln^4(\mu), \quad \mu = \frac{g z_0}{c_p^2} e^{\kappa/x} \leq 1, \tag{7}$$

where $\beta_m = 1.2$ determines the overall strength of S_{in}, $\kappa = 0.41$, g=9.81 m/s^2.

A.2 The white-capping dissipation

$$S_{\text{dis}} = -C_{\text{dis}} < \omega > \left(\frac{\alpha}{\alpha_{\text{PM}}} \right)^{D_s} \left\{ (1 - \delta) \left(\frac{k}{< k >} \right) + \delta \left(\frac{k}{< k >} \right)^2 \right\}, \tag{8}$$

where

$$\alpha = E < k >^2 \tag{9}$$

is the square of the average steepness of the spectrum and $\alpha_{\text{PM}} = 4.57 \times 10^{-3}$. The symbol $< \cdot >$ is related to an average over the wave spectrum F. In WAM cycle 4 the values D_s=2, δ=0.5 and an overall strength $C_{\text{dis}} = 9.4 \times 10^{-5}$ are used.

A.3 The nonlinear interaction

$$S_{\text{nl}}(1) = C_{\text{nl}} \sum_{\text{quadruplets}} C(1, 2, 3, 4) F(2) F(3) F(4). \tag{10}$$

Here $C_{\text{nl}} = 1$ is a normalising factor, 1, 2, 3 and 4 denote the individual members of a wave quadruplet. The cross section $C(1, 2, 3, 4)$ is only nonzero for resonating quadruplets:

$$\mathbf{k}_1 + \mathbf{k}_2 = \mathbf{k}_3 + \mathbf{k}_4, \qquad \omega_1 + \omega_2 = \omega_3 + \omega_4. \tag{11}$$

A.4 The bottom dissipation

$$S_{\text{bot}} = -2 \frac{C_{\text{bot}}}{g} \frac{k}{\sinh(2kd)} F. \tag{12}$$

Here d is the local water depth. The normalising factor C_{bot} depends on the nature and structure of the sediment. In WAM cycle 4 the value C_{bot}=0.038 (JONSWAP) is used.

References

Barzel G., 1994. Optimierung eines seegangsmodells mit der adjungierten methode, (MPI Examsarbeit; 26). Available at Max-Planck-Institut für Meteorologie, Hamburg.

Burgers G., Leeuwen van P. J. and G. Evensen, 1998. Analysis Scheme in the Ensemble Kalman Filter. *Mon. Wea. Rev.*, **126**, 1710-1724.

Evensen G., 1997. Advanced data assimilation for strongly nonlinear dynamics. *Mon. Wea. Rev.*, **125**, 1342-1354.

Giering, R. and Kaminski, T, 1997. 'Recipes for Adjoint Code Construction'. to appear in *ACM Trans. On Math. Software.*

Gilbert J. Ch., C. Lemaréchal, 1989. 'Some numerical experiments with variable-storage quasi-Newton algorithms' *Mathematical Programming*, **45**, 407-435.

Hasselmann, K., T. P. Barnett, E. Bouws, H. Carlson, D. E. Cartwright, K. Enke, J. A. Ewing, H. Gienapp, D. E. Hasselmann, P. Kruseman, A. Meerburg, P. Müller, D. J. Olbers, K. Richter, W. Sell and H. Walden, 1973. Measurements of wind-wave growth and swell decay during the Joint North Sea Wave Project (JONSWAP), *Dtsch. Hydrogr. Z. Suppl. A* **8(12)**, 95p.

Heras, M. M. de las and P. A. E. M. Janssen, 1992. Data assimilation with a nonlinear, coupled wind wave model. *J. Geophys. Res.* **C97**, 20261-20270.

Heras, M. M. de las, G. J. H. Burgers and P. A. E. M. Janssen, 1994. Variational data assimilation in a third generation wave model. *J. Atmos. Ocean. Techn.* **11**, 1350-1369.

Hersbach H., 1997. The adjoint of the WAM model, KNMI-WR internal report. Available at KNMI, The Netherlands.

Hersbach H., 1998. Application of the adjoint of the WAM model to inverse wave modeling. *J. Geophys. Res.* **103**, 10469-10487.

Hersbach H. and P. A. E. M. Janssen, 1999, Improvement of the Short Fetch Behavior in the WAM model. *J. Atmos. Ocean. Techn.* **16**, 884-892.

Janssen, P. A. E. M., 1989. Wave-induced stress and the drag of air flow over sea waves. *J. Phys. Oceanogr.* **19**, 745-754.

Janssen, P. A. E. M., 1991. Quasi-linear theory of wind wave generation applied to wave forecasting. *J. Phys. Oceanogr.*

Kahma, K. K. and C. J. Calkoen, 1992. Reconciling discrepancies in the observed growth of wind-generated waves. *J. Phys. Oceanogr.* **22**, 1389-1405.

Kållberg, P., 1990. The HIRLAM forecast model, level 1, documentation manual, Swedish Meteorol. and Hydrol. Inst., Norrköping, Sweden.

Komen, G. J. et al, *Dynamics and Modelling of Ocean Waves*, Cambridge University Press 1994.

A. J. Kuik, G. Ph. van Vledder and L. H. Holthuijsen, 1988. A method for the Routine Analysis of

Pitch-and-Roll Buoy Wave Data, *J. Phys. Oceanogr.* **18**, 1020-1034.

Pierson, W. J.,Jr. and L. Moskowitz, 1964. A proposed spectral form for fully developed wind seas based on the similarity theory of S.A. Kitaigorodskii. *J. Geophys. Res.* **69**, 5181.

Rabier. F., H. Jarvinen, E. Klinker, J.F. Mahfouf, and A. Simmons, 2000: The ECMWF operational implementation of four dimensional variational assimilation. Part I: Experimental results with simplified physics. *Quart. J. Roy. Meteor. Soc.*, **126**, 1143-1170.

Valk, C. F. de, and C. J. Calkoen, 1989. Wave data assimilation in a third generation wave prediction model for the North Sea - An optimal control approach. Delft Hydraulics Laboratory, report X38, Delft, 123p.

Young, I and L. A. Verhagen, 1996. The growth of Fetch Limited Waves in Water of Finite Depth. part I and II. Submitted to Coastal Engineering.